International Letters of Chemistry, Physics and Astronomy *Online: 2015-07-01*
ISSN: 2299-3843, Vol. 53, pp 71-78
doi:10.18052/www.scipress.com/ILCPA.53.71

Studies on structural, morphology and electrical properties of chemically sprayed WO_3- V_2O_5 nanocomposites thin films

J. M. Patil[*a], S. B. Patil[b], R. H. Bari[b], A. N. Sonar[a]

[a*]Department of Chemistry, Shri. V. S. Naik, A.C.S. College, Raver, 425508, Maharashtra, India.

[b]Nanomaterials Research Laboratory, Department of Physics, G. D. M. Arts, K. R. N. Com. And M. D. Science College, Jamner, 424 206, Maharashtra, India.

E-mail address: jmpatil799@gmail.com

Keywords: Spray Pyrolysis, WO_3-V_2O_5 nanocomposites, XRD, activation energy.

ABSTRACT. Spray pyrolysis technique was employed to prepare WO_3-V_2O_5 nanocomposites thin onto the preheated glass substrate at 350 ^oC. The films were characterized using X-ray diffractogram (XRD), Field emission scanning electron microscopy (FE-SEM), and Element composition was studied using energy dispersive spectrophotometer (EDAX).The film thickness was measured using weight difference method. Electrical conductivity measured with the help of two probe method. The crystallite size and grain size were observed to be increase with increase in films thickness with decrease in activation energy. The results are discussed and interpreted.

1. INTRODUCTION

Semiconductors metal oxides are used extensively as a sensing element of different gases and vapors. A depletion region always formed at the surface of metal oxide semiconductor due to adsorption of air oxygen molecules. Then the reaction with the target gas molecule causes reduction of depletion region which results change in conductivity of metal oxide semiconductor. The conductivity may increase or decrease depending on type of semiconductor and type of target gas [1-2].

Tungsten oxide (WO_3) is a transition metal oxide semiconductor with a widely band gap, in the range of Eg=2.5-2.8eV at room temperature. Interest was recently put on WO_3 thin films and nanoparticles [3]. WO_3 is n-type semiconductor that encloses interesting physical and chemical properties, that is why it is useful for a wide spectrum of technologies applications. For instance, tungsten oxide is an important material for electrochromic [4] and photoelectrochemical devices [5], catalyst [6] and gas sensors [7, 8].

Vanadium pentoxide is generally a non-stoichiometric material, which is known for its catalytic properties in oxidation reactions. Moreover, their use as components of gas sensors has been proposed [9]. The electrical transport mechanism in V_2O_5 fibres have been studied in detail [10]. V_2O_5 is an *n*-type semiconductor with an electronic conductivity in the order of 0.5 Scm^{-1} at room temperature [11].

The metal oxide-sensing layer (WO_3 or V_2O_5*)* has been fabricated in different physical forms such as thin film, thick films, and bulk pellets. However, the thin film form is expected to be most effective, because sensing is basically a surface phenomenon of film [12-13]. Thus, a very few work has been reported for the combination of WO_3/V_2O_5 oxide composite [14].

However, not much attention has been given to the fabrication of nanocomposites thin films. There has been intensive research on improving the gas sensitivity and selectivity by controlling the particle size [15, 16], nanostructures [17, 18], sensing temperature [19], surface and structure [20].

Spray pyrolysis has proved to be simple, reproducible and inexpensive, as well as suitable for large area applications. Besides the simple experimental arrangement, high growth rate and mass production capability for large area coatings make them useful for industrial as well as solar cell applications. In addition, spray pyrolysis opens up the possibility to control the film morphology and particle size in the nanometer range [21].

In this work, WO_3-V_2O_5 nanocomposites thin films with different volume ration of precursor were prepared by spray pyrolysis technique. The films were characterized using different analytical techniques. The results were discussed and interpreted in the present investigations.

2. EXPERIMENTAL DETAILS

2.1 Substrate cleaning

The substrate cleaning is very important in the deposition of thin films. Commercially available glass slides with a size of 25 mm × 25 mm × 1 mm were washed using soap solution and subsequently kept in hot chromic acid and then cleaned with deionized water followed by rinsing in acetone. Finally, the substrates were previously cleaned with deionized water for 20 min and wiped with acetone and stored in a hot oven.

2.2 Preparation of pure WO_3, V_2O_5, and WO_3-V_2O_5 nanocomposites thin films

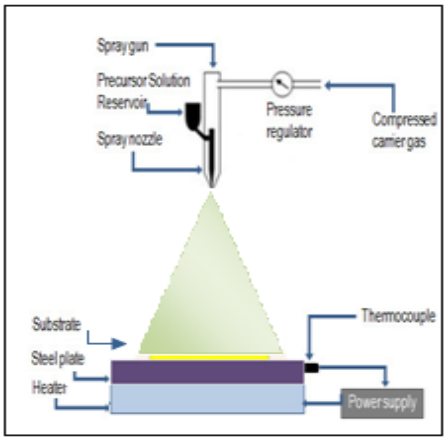

Fig. 1. Schematic diagram of spray pyrolysis system for the preparation of WO_3, V_2O_5, and WO_3-V_2O_5 nanocomposites thin films

Fig. 1 shows spray pyrolysis technique for preparation of WO_3-V_2O_5 nanocomposites thin films. Set-up consists of spraying chamber, spray nozzle (gun), compressor for carrier gas, heating system, and temperature indicator.

2.3 Preparation of WO_3-V_2O_5 nanocomposites thin films

The starting material used for the preparation of WO_3-V_2O_5 nanocomposites thin films were tungsten hexachloride (WCl_6, Purified Merck) and vanadium (III) chloride (VCl_3), Purified Aldrich). Tungsten hexachloride and vanadium (III) chloride were mixed at various volume ratio such as 30:70, 50:50 and 70:30 as indicated in Table 1.

Table 1: Amounts of spraying solutions and reactant

Sample No.	WCl_6 (cm^3)	VCl_3 (cm^3)	Reactants
S1	30	70	WO_3:V_2O_5
S2	50	50	WO_3:V_2O_5
S3	70	30	WO_3:V_2O_5

The optimized deposition parameters like substrate temperature (350 ^oC), spray time (10 mn.), rate of spraying solution (8 ml/min.), nozzle to substrate distance (30 cm), quantity of the solution sprayed (30 ml), pressure of carrier gas, and to and fro movement of the nozzle were kept constant. The temperature of the substrate is maintained at a constant value by using a temperature

controlled hot plate. The film formation depends upon the droplet landing, reaction and solvent evaporation, which relates to the droplet size. When the droplet approaches the substrate just before the solvent is completely removed, that is the ideal condition for the preparation of the WO_3-V_2O_5 nanocomposites thin film.

2.4 Post preparative treatment

The as prepared WO_3-V_2O_5 nanocomposites thin films samples (S1, S2, and S3) were annealed at 500 ^oC for 1 h.

3. CHARACTERIZATIONS OF THIN FILMS

The film thickness was measured by a well-known weight difference method. The pure WO_3, V_2O_5, and WO_3-V_2O_5 nanocomposites thin films were characterized by X-ray diffraction (Miniflex Model, Rigaku, Japan)) using CuKα radiation with a wavelength, λ = 1·542 Å. The surface morphology and elemental composition of the thin films were analyzed using Field emission scanning electron microscope (FE-SEM, Hitachi S 4800) coupled with energy dispersive spectrophotometer (EDAX).Electrical property measurement was studied by using two probe resistivity set up.

4. RESULTS AND DISCUSSION

4.1. Determination of film thickness

The film thickness was measured by a well-known weight difference method [22] in which weight of the sample, area and densities were considered. The thickness, sample weight and sample area are related as:

$$t = M/A.\ \rho \quad (1)$$

Where, M is the weight of the sample in gm,
A the area of the sample in cm^2
and ρ the materials density in $gm\ cm^{-3}$.

The values of the film thickness with crystalline size are given in Table 3.

4.2. Structural analysis using X-ray diffractogram

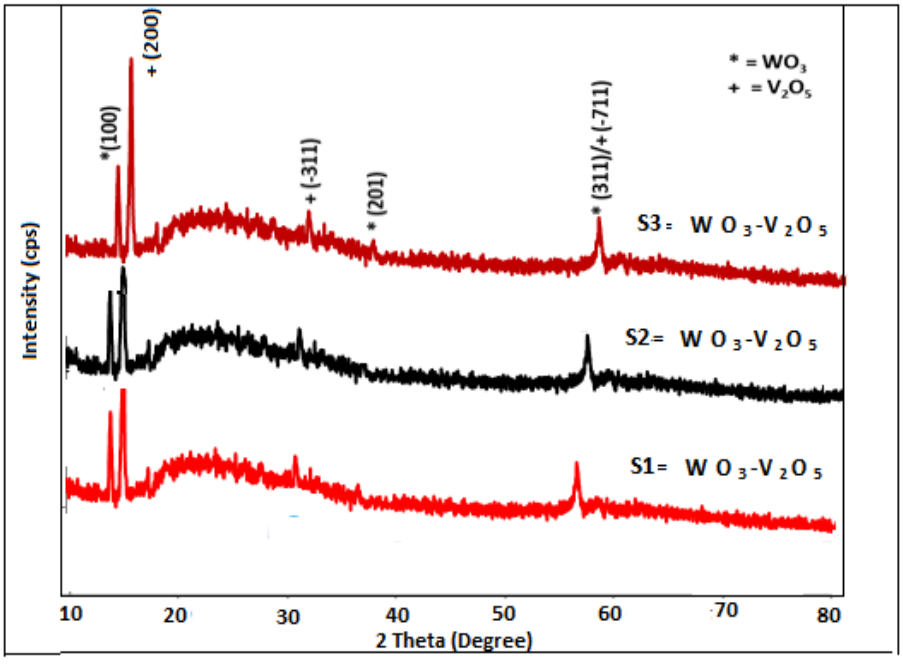

Fig. 2. X-ray diffractogram of WO_3-V_2O_5 nanocomposites thin films samples: (a) S1, (b) S2,and (c) S3

The crystal structures of mixed WO_3 – V_2O_5 nanocomposites thin films obtained were characterized by X-ray diffractogram (XRD). Fig. 2 shows the X-ray diffractogram of thin film samples S1, S2, and S3. The 2θ values were varied from 10 to 80^O. The XRD patterns of WO_3 indicate hexagonal structure and V_2O_5 shows monoclinic structure. Sample S1- S3 indicates mixed phases of WO_3 (*) and V_2O_5 ($^+$). No other impurities was observed in XRD. XRD pattern revealed that (for sample S3-S5) the formation of WO_3-V_2O_5 nanocomposites thin films. The WO_3 and V_2O_5 diffraction peaks are match with standard ASTM data WO_3 and V_2O_5 [23-24]. The observed peak predominates indicating a preferential growth. This means that the grains have *c*-axis perpendicular to the substrate surface. The average crystallite size of WO_3-V_2O_5 nanocomposites thin film samples were calculated by using the Scherrer formula.

$$D = 0{\cdot}9\lambda/\beta\cos\theta \quad (2)$$

Where, D = Average crystallite size
λ = X-ray wavelength (1·542 Å)
β = FWHM of the peak
θ= Diffraction peak position.

The calculated average crystallite sizes were presented in Table 3.

4.3. Surface Morphology

4.3.1. Field emission scanning electron microscope

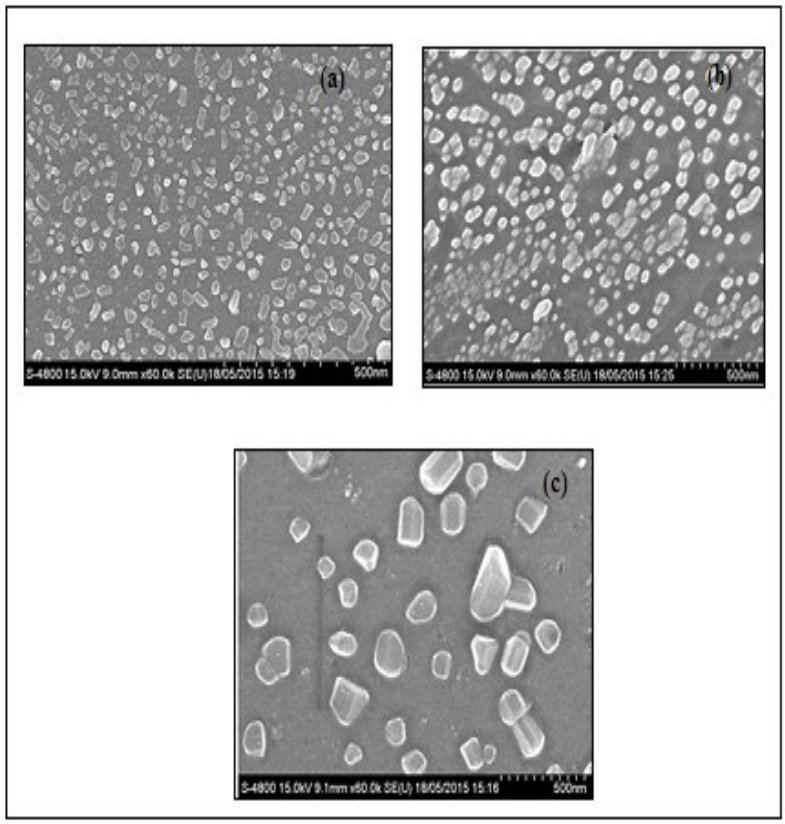

Fig.3. FE-SEM images pure WO_3, V_2O_5, and WO_3-V_2O_5 nanocomposites thin films: (a) S1, (b) S2, (c) S3 (d) S4 and (e) S5

FE-SEM images of WO_3-V_2O_5 nanocomposites were represented in Fig.3. Fig. 3 (a) shows the angular formation of the grain for WO_3 and for V_2O_5 grains were observed to be spherical in shape with different size. By increasing WO_3 % in V_2O_5 (Fig.3(a) (b) and (c)) thin films, the shape of the grains change into the mixed cubical and monoclinic phases. Grain size observed to be in the range of 21 - 44 nm.

4.4. Elemental composition using (EDAX)

The quantative element compositions of the thin film samples were analyzed using an energy dispersive spectrometer. Stoichiometrically expected at % for WO_3-V_2O_5 is : 9.09, 18.18 and 72.72, Observed at % for WO_3, V_2O_5, and WO_3-V_2O_5 nanocomposites thin films were given in Table 2.

Table 2: Quantative elemental analysis as prepared pure WO_3-V_2O_5 nanocomposites thin film

Element	Observed					
	S1		S2		S3	
	mass %	at %	mass %	at %	mass %	at %
W	10.24	01.49	45.25	10.87	51.37	09.01
V	44.91	23.57	32.73	28.37	05.07	25.21
O	44.85	74.94	22.02	60.71	43.56	65.78
Total	100	100	100	100	100	100

It is clear from table 2, that as prepared WO_3-V_2O_5 nanocomposites thin films were observed to be nonstoichiometric in nature. Sample S2 was observed to be more oxygen deficiency as compared to other samples.

4.5. Electrical properties

4.5.1. Electrical conductivity

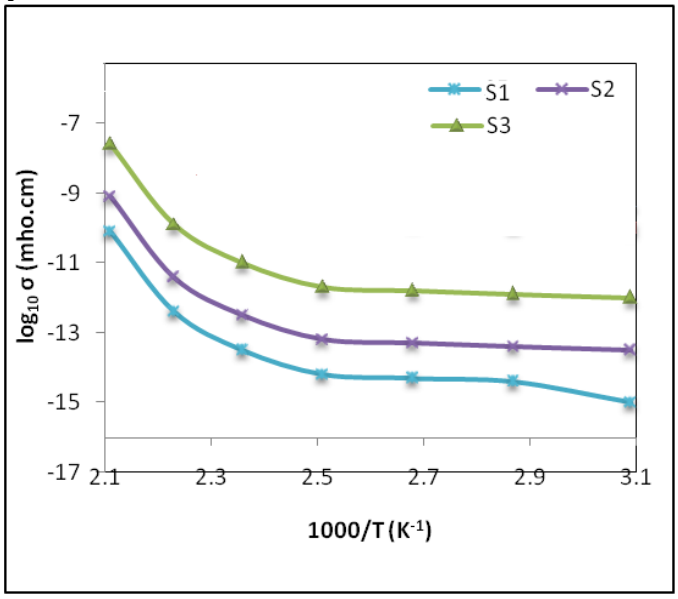

Fig. 4. Variation of log (σ) with operating temperature (◦C).

Fig. 4 shows the variation of log (σ) with operating temperature. The conductivity of each sample is observed to be increasing with an increase in temperature. The increase in conductivity with increase in temperature could be attributed to negative temperature coefficient of resistance and semiconducting nature of the films. It clearly indicates that the WO_3, V_2O_5, and WO_3-V_2O_5 nanocomposites thin films are semiconducting in nature [25].

The thickness of the film was varied from 113 to 163 nm. It was found that the thickness of the film increases with increase of at % W in V_2O_5. It is also clear from table 3, that crystallite and grain size goes on increasing with increase in film thickness and mass % of W in V_2O_5.

Table 3: Measurement of film thickness with crystalline and grain size

Sample No.	Thickness (nm)	Crystallite size calculated from XRD (nm)	Grain size observed from FE-SEM (nm	Activation energy ($\triangle$ E)	
				50 ^{O}C	200 ^{O}C
S1	140	27	39	0.48 eV	0.44eV
S2	156	29	41	0.46 eV	0.38eV
S3	163	33	44	0.37 eV	0.31eV

It is reported [26, 27] as the thickness of the film increases activation energy goes on decreasing. Electrical conductivity was calculated using the relation:

$$\sigma = \sigma_o \exp(-\Delta E/kT) \quad (3)$$

Where, σ = conductivity

σ_o = conductivity constant

k = Boltzmann constant

T = Temperature

In Table 3 the activation energy is calculated from slopes of line for sample S1, S2, and S3 thin films. It is clear from Table 3 that, as film thickness of the sample goes on increasing; the activation energy goes on decreasing. The decrease in activation energy with increasing film thickness may be due to the change in structural parameters, improvement in crystalline and grain size [28].

5. CONCLUSIONS

- Nanocomposites WO_3-V_2O_5 thin films were prepared by simple and inexpensive spray pyrolysis technique.
- The physical, structural, and surface morphological properties confirm that the as-prepared WO_3-V_2O_5 thin films are nanocrystalline in nature.
- The elemental analysis conferred that as prepared thin films were nonstoichiometric in nature.
- The average crystallite size and grain size was observed to be increase with increase in
- films thickness.
- Electrical conductivity of the nanocomposites WO_3-V_2O_5 thin films were observed to be increased with increase in temperature.
- As the thickness of the films goes on increase, activation energy goes on decreases.

Acknowledgements

The authors are thankful to the University Grants Commission, New Delhi for providing financial support. Thanks to Principal, Shri. V. S. Naik A.C.S. College, Raver, for providing necessary infrastructure laboratory facilities for this work. I have also appreciate Prof. Dr. R. H. Bari, Head of Department, Department of Physics, G. D. M. Arts, K. R. N. Com. And M. D. Science College, Jamner for their help. We thanks NMU, Jalgaon for the motivation and encouragement for giving me the opportunity to do this research work as successful one.

Reference

[1] L. Ottaviano, L. Lozzi, M. Passacantando, and S. Santucci, *Surface Science*, 475 (2001) 73-82.

[2] L. J. LeGore, R. J. Lad, S. C. Moulzolf, J. F. Vetelino, B. G. Frederick, and E. A. Kenik, *Thin solid films*, 406 (2002) 79- 86.

[3] N. Soultanidis, W. Zhou, Ch.J. Kiely, and M.S. Wong, *Langmuir*, 28 (2012)17771-17777.

[4] C. G. Granqvist, *Solar Energy Materials & Solar Cells*, 60 (1999) 201-262.

[5] A. Di Paola, L. Palmisano, A. M. Venezia, and V. Augugliano, *J. Phys. Chem. B*, 103(1999) 8236-8244.

[6] A. Löfbeg, A. Frennet, G. Leclercq, L. Leclercq, and J. M. Giraudon, *Journal of Catalysis*, 189 (2000) 170-183.

[7] G. Eranna, B. C. Joshi, D. P. Runthala, and R. P. Gupta, *Critical reviews in Solid State and Materials Sciences*, 29 (2004) 111-188.

[8] P. J. Shaver, *Appl. Phys. Lett.,* 11 (1967) 255-256.

[9] U. Schlecht, I. Besnard, A. Yasuda, T. Vossmeyer, M. Burghard, in: H. Kuzmany, J. Fink, M. Mehring, S. Roth (Eds.), *American Institute of Physics*, Melville, NY, CP685, (2003), 491.

[10] J. Muster, G.T. Kim, V. Krstic, J.G. Park, Y.W. Park, S. Roth, M. Burghard, *Adv. Mater.,* 12 (2000) 420–424.

[11] G.T. Kim, J. Muster, V. Krstic, J.G. Park, Y.W. Park, S. Roth, M. Burghard, *Appl. Phys. Lett.* 76 (2000) 1875–1877.

[12] P. Mitra and A.K. Mukhopadhyay, *Bull. Of the Polish Academy of Sciences Technology*, 55, (2007) 281-285.

[13] M.K. Hossain, S.C. Ghosh, Y. Boontongkong, C. Thanachaynont and J. Dutta, *Journal of Metastable and Nanocrystalline materials*,23(2005) 27-30.

[14] P.R. Makgwane , S.S. Ray, *Catalysis Communications*, 54 (2014) 118–123.

[15] N. Yamazoe, *Sens.Actuators B*, 108 (2005) 2-14

[16] C.N. Xu, J. Tamaki, N. Miura, N. Yamazoe, *Sens. Actuators B,* 3 (1991) 147-155.

[17] E. Comini, G. Faglia, G. Sberveglieri, Z. Pan, Z.L.Wang, *Appl. Phys. Lett*., 81 (2002)1869-1871.

[18] Y. Wang, X. Jiang, Y. Xia, A solution-phase, *J. Am. Chem. Soc.,* 125, (2003)16176-16177.

[19] A. Chiorino, G. Ghiotti, F. Prinetto, M.C. Carotta, D. Gnani, G. Marinelli, *Sens. Actuators B*, 58 (1999) 338-349.

[20] Y. Shimizu, E.D. Bartolomeo, E. Traversa, G. Gusmano, T. Hyodo, K. Wada, M. Egashira, *Sens. Actuators B* ,60 (1999)118-124.

[21] R. H. Bari, S. B. Patil, A.R. Bari, G. E. Patil, J. Aambekar, *Sensors & Transducers*,140, (2012) 124-132.

[22] V. B. Patil, G. S. Shahane and L. P. Deshmukh, *Materials Chemistry and Physics*, 80, (2003) 625-631.

[23] JCPDS card no. 01-075-2187

[24] JCPDS card no.00-054-0513.

[25] G. E. Patil, D. D. Kajale, D. N. Chavan, N. K. Pawar, P. T. Ahire, S. D. Shinde, V. B. Gaikwad, *Bull. Mater. Sci*., 34 (2011) 1-9.

[26] K.C. Sharma, J.C. Garg, *Physic D: Applied Physics,* 23(1990) 1411.

[27] Z.S. EL-Mandouh, M. EL-Shabasy*, Fizikaa,* A4 (1995), 17.

[28] R. H. Bari, S. B. Patil, A. R. Bari, *Optoelectronics and advanced materials–rapid communication,* 6 (2012) 887-895.